CONF 841218--30

UCRL--90922

DE87 008732

MARS - Mirror Advanced Reactor Study

B. Grant Logan

This paper was prepared for submittal to:
The Journal of Vacuum Science and Technology

September 10, 1984

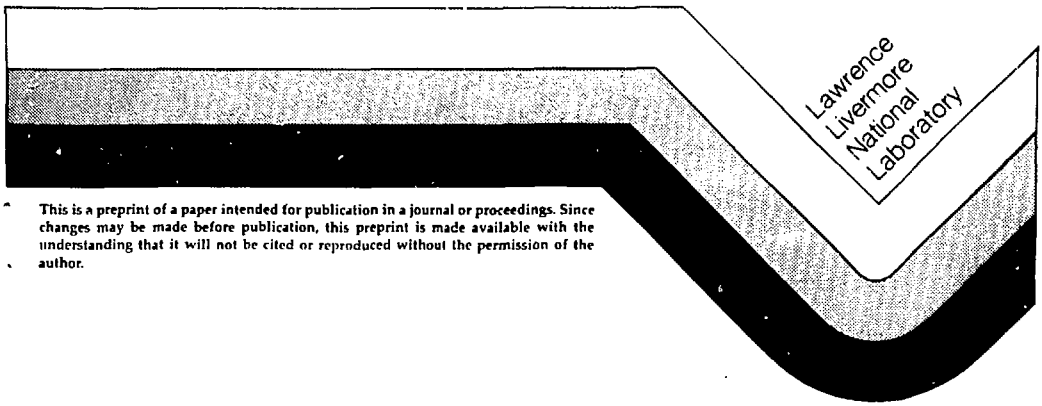

MARS - MIRROR ADVANCED REACTOR STUDY

B. G. Logan

Lawrence Livermore National Laboratory

University of California

P. O. Box 808

Livermore, CA 94550

ABSTRACT

A recently completed two-year study of a commercial tandem mirror reactor design [Mirror Advanced Reactor Study (MARS)] is briefly reviewed. The end plugs are designed for trapped particle stability, MHD ballooning, balanced geodesic curvature, and small radial electric fields in the central cell. New technologies such as lithium-lead blankets, 24T hybrid coils, gridless direct converters and plasma halo vacuum pumps are highlighted.

---

*Work performed under the auspices of the U.S. Department of Energy by the Lawrence Livermore National Laboratory under contract number W-7405-ENG-48.

INTRODUCTION

The Mirror Advanced Reactor Study (MARS) [1] is a recently completed two-year study of a commercial tandem mirror reactor, conducted by the Lawrence Livermore National Laboratory for the U.S. Department of Energy, with TRW as the prime industrial partner, General Dynamics, EBASCO and Science Applications, Inc. (SAI, La Jolla, CA) as subcontractors, and the University of Wisconsin as a university partner. Grumman Aerospace Corp. has also contributed a significant portion of the engineering effort. The main objectives of the MARS study were to design an attractive reactor incorporating both physics and technology constraints, to identify key new physics and technologies which will need testing and development for reactors, and to find ways of exploiting the potential of fusion for safety, low activation, and simple disposal of radioactive waste. To keep this review brief, only a condensed description of the MARS design is presented, focusing mainly on power balance, direct conversion, and end plug magnet design.

OVERALL DESCRIPTION OF MARS

MARS (Figs. 1, 2) is a linear tandem mirror fusion reactor using electrostatic plugs of the thermal barrier type [2,3] to confine a steady state fusion plasma in a 130 meter long solenoid (cross-section shown in Fig. 3) producing 2600 MW of fusion power. TABLE I summarizes key MARS reactor parameters. The central cell is fueled with DT pellets, and with $\Phi_{plug}-\Phi_{central\ cell} \simeq 150$ kV ion

confining potentials, fusion alpha heating sustains nearly all central cell axial and radial energy losses totaling ∿ 500 MW; i.e., the central cell is "ignited." The plugs require continuous injection of about 100 MW total, mostly ECRH (TABLE I), so Q ≡ fusion power/plug injection power ≈ 26 for MARS, and would scale approximately linearly with central cell length and fusion power. DT fuel ions and thermalized alpha ash escape mainly by radial diffusion via drift-pumping into an unplugged diverted flux annulus (called a "halo"), which serves both for impurity removal and vacuum pumping. The electrons escape mainly along the field lines by energy diffusion, collected on end wall plates biased ∿ -7 T_{ec} negative with respect to the halo (ground) potential. Because of the non-ambipolar radial loss of ions, this simple form of direct conversion does not require grids to separate ion and electron currents, and also serves to minimize radial electric fields in the central cell as required for MHD stability and moderate resonant radial transport. The directly recovered electron energy amounts to half of all the plasma energy losses, and supplies most of the total reactor plant recirculating electric power of 336 MWe in TABLE I, for a cost per kilowatt less than conventional turbine-generators. Thus, with a blanket neutron-energy multiplication of 1.36 and a thermal cycle efficiency of 40% using a novel liquid metal eutectic $Li_{17}Pb_{83}$ as both coolant and tritium breeder, MARS can produce a net electric power of 1200 MWe, nearly half of the fusion power. Smaller net power reactors would be possible without sacrificing this overall efficiency by lowering the wall neutron loading below the high 4.3 MW/m^2 MARS value.

Note that, due to high beta and fusion power density, the plasma radius in MARS is only 0.5 meters in both the central cell and in the plugs where the average field is about the same as in the central cell (≈ 4 T). Due to the plasma diversion in the halo, first wall surface heating is low (< 4 watts/cm^2), allowing the first wall to be placed close to the plasma (see Fig. 3). The net result of this is that the superconducting magnets in MARS have a characteristic radial dimension of 3 meters (both solenoids and yin yang coils) as opposed to 6 to 8 meters in Tokamak toroidal field coils. Smaller radius results in lower average stresses in the superconductor

$$\sigma(\text{Pascals}) = j_{Ave}(A/m^2)\ r_{coil}(m)\ B_{conductor}(T)$$

permitting either cheaper conductors or higher current densities with lower magnet weight. For the same reasons, the small plasma radius in MARS allows a small bore (r_{coil} = 9.3 m) in the high field choke coils (Fig. 4) at the ends of the central cell, so that 24 T fields are possible at stress levels compatible with current materials.

The MARS study has also made significant advances in the areas of safety and activation which will be as important as physics in the success of fusion. Due to the low solubility of T_2 in the $Li_{17}Pb_{83}$ eutectic, the entire inventory of tritum in the MARS blanket is less than 5 grams (> 100 grams could result in > 25 rem dose at the plant boundary in accident situations). Elimination of cryopanels in favor of halo pumping keeps the vulnerable tritium in the vacuum

system to less than about 10 grams. The ferritic steel alloys used in the first wall and blanket will not melt due to afterheat if there were a prompt loss of either coolant or flow. The low nickel and molybdenum steel alloys used in MARS also meet the U.S. Nuclear Regulatory Commission's rules (10CFR61) for on site, near surface land burial. Thus, radioactive waste generated in MARS ($\sim$ 100 tons/year) need not be processed and transported long distances to high level repositories, but simply buried on site. Almost all the radioactivity decays with 5 year half-life.

MARS END PLUG DESIGN

Figure 5 shows the MARS end plug magnets (a) together with the magnetic field and plasma potential profiles along the z axis (b), and the associated contour plot of $\phi(r,z)$(c). The end magnets consist of a high field hybrid solenoid (the 24 T choke coil of Fig. 4) followed by two back-to-back yin yang mirror wells with Cee coils on each end to recircularize the flux tube going into the central cell and into the direct converter. The outermost yin yang mirror well contains neutral-beam injected sloshing ions, mirror trapped hot electrons and warm electrons heated by ECRH to form a thermal barrier "plug" as in TMX-Upgrade. ICRH heating in the inner yin yang mirror well, called an "anchor", provides most of the MHD stability for the system. The entire region between the choke coil B-peak and the plug potential peak is kept at a low density relative to the central cell ($n_{plug}(z) \approx n_c \, B_{plug}(z)/B_{max}$) by radial loss induced by the drift pumping. Plots of the normal and geodesic curvatures

associated with the magnet design in Fig. 5 are shown in Figs. 6 and 7, respectively. End plug plasma parameters are given in TABLE II.

The m = 1 ballooning beta limit as calculated by the LLNL equilibrium and stability code TEBASCO [4] is $\langle\beta_c\rangle \simeq 0.28$ with $(r_{wall} - r_{plasma})/r_{plasma} = 0.65$, effectively, in the transition regions. As ballooning and interchange beta limits are both roughly proportional to B_{max}, both central cell wall loading and the reactor Q increase with B_{max}. For high central cell beta it is also important to have the ICRH heated anchor; without ICRH creating mirror-confined hot ion pressure in the anchor, the interchange beta limit would drop about a factor of three, and the ballooning beta limit by about an order of magnitude due to increased bending through the two elliptical fans.

The trapped particle mode stability for the worst m = 1 mode requires [5]

$$\frac{\omega_{*i}^2}{\gamma_c^2} > \frac{4(1 + A)}{A^2}$$

where $A \simeq \left(\frac{r_c}{\rho_i}\right)^2 \frac{n_{pass}}{n_c} \frac{B_c}{B_t} \frac{2L_t}{L_c}$

For MARS, $\omega_{*i} \sim \gamma_c$, requiring $A > 4.8$ for stability. With $r_c/\rho_i \simeq 60$ and $L_t \simeq 20$ m, $L_c \simeq 130$ m, we need

$$\frac{n_{pass}}{n_c}\ \frac{B_c}{B_t} \approx \frac{B_c}{B_{max}}\qquad \frac{T_{ic}}{\pi\delta\Phi_t} > 4 \times 10^{-3}$$

or $B_{max} < 100\ B_c$. Thus, B_{max} is unlikely to be limited by trapped particle stability, but rather will be limited by practical coil designs.

The geodesic curvature shown in Fig. 7 averages to zero for central cell ions and electrons passing through and reflecting off the potential barriers at the ends, and also nearly averages to zero for ions and electrons locally trapped in the anchors and plugs (local omnigeneity). Since the central cell is close to ground (halo) potential, the transitions, anchors and plugs have negative radial electric field ($\Delta\phi_r \approx -20$ kV). The local bounce average ExB drifts are small enough in MARS that the radial drifts of ions passing through the two peaks in Fig. 7 are well canceled, to within a couple percent. This results in estimated neoclassical "boundary layer" central cell ion transport which is an order of magnitude smaller than the induced drift-pumping current in MARS.

MARS DRIFT PUMPING

The region between the magnetic field (B) and potential (ϕ) peaks of the thermal barrier plugs must operate at lower potential and density relative to the central cell (see Fig. 5). Collisions of central cell ions passing through these regions generate trapped ions that must be continuously pumping, that is, inducing radial loss of the trapped ions by means of low frequency (50-kHz) RF fields [6]. Long, hairpin-shaped, drift-pump coils generate perpendicular per-

turbation fields ($B \sim 0.04$ T) in the end cell ellipses causing non-cancelled geodesic curvature and radial drifts. Matching these drift-pump coil frequencies to trapped-ion bounce frequencies causes radial diffusion of the unburned DT fuel, thermalized alpha ash, and other impurities to the unplugged plasma edge where they divert into annular "halo" dumps in the direct converter (Fig. 2). Faster bouncing electrons are left to escape along field lines to the negatively biased electron collectors inside the halo dumps.

With sufficient potential barriers to suppress axial ion leakage, the radial drift pumping of the central cell ions trapped in the end cells becomes the dominant cause of central cell plasma and energy losses. Then ignition in MARS requires a minimum central cell length--several times the end cell length (L_T in Fig. 5)--for alpha heating to balance the loss from ions trapped in the end cells. A central cell shorter than the MARS version would require either auxiliary central cell heating or reduced end cell size.

MARS REACTOR COSTS

Fig. 8 outlines component direct costs of the tenth-of-a-kind MARS reactor plant (the nuclear island portion of the total power plant). The total cost of the island is 1.52×10^9 \$US. Magnet costs clearly dominate, reflecting their mass (16,800 t of magnets and associated structure from 26,000 t of total reactor weight). End cell portions of the cost (the unshaded areas in Fig. 8) constitute about half of the total reactor plant costs. Furthermore,

this total reactor plant cost is more than half of the total power plant direct cost: 2.37×10^9 $US. Total capital costs--including engineering, construction, interest, and escalation--are almost double the direct costs. Note that these costs are given for the tenth-of-a-kind reactor, about 16% less than those for the first reactor.

NEW DIRECTIONS

Clearly, future work in tandem mirror reactor design should seek ways to reduce magnet size and weight. Engineering solutions to double the average current density of winding ($1.8 \times 10^7 A/m^2$ in MARS) and reduce the required shield thicknesses may be found. In addition, larger gains could result from reducing the end cell size. The length of the MARS end cells derives from quadrupole physics requiring six C-coils, but the fundamental minimum length needed for ion adiabaticity is three times shorter, as illustrated by the MINIMARS configuration in Fig. 9. Correspondingly, the minimum central cell length for ignition could be shorter, permitting smaller reactors. Several approaches to achieving MHD stability of such compact systems are currently being examined, including octupole magnets (shown in Fig. 9, relativistic electron rings, RF ponderomotive fields, and conducting wall effects.

TABLE I. Characteristic MARS Parameters.

Central cell length	130 m
Plasma radius	0.49 m
Fusion power	2600 MW
Ave. central beta $<\beta_c>$	28%
Peak central density	3.3×10^{20} m^{-3}
T_{ic} = 28 keV	
T_{ec} = 24 keV	
Solenoid field	4.7 T
Peak choke coil field	24 T (15 T SC+9 T Cu insert)
Yin-yang mirror field	7.5 T (10 T on conductor)
First wall loading	4.3 MW/m^2 (r_{wall} = 0.6 m)
Blanket coolant - breeder, temp., & power multiplication	$L_{17}Pb_{83}$, 500°C, M = 1.39
Plug neutral beam absorbed	3.0 MW each plug
Plug ECRH absorbed	42 MW each plug
Anchor ICRH absorbed	5 MW each anchor
Copper coil power (inserts and drift pumps) power	50 MWe each plug
Total recirculating power	336 MWe
Direct converter power (total)	290 MWe
Net electric power produced	1200 MWe
Recirculating power fraction	0.22
Magnet stored energy (total)	49 GJ
Efficiencies	
Direct converter	0.50
475 kV sloshing ion beams	0.60
ECRH 0.65	
Anchor ICRH	0.50
Thermal cycle	0.40
Overall system (plant)	0.36

TABLE II. MARS End Cell Parameters.

Transition/anchor	
Length	13.3 m
Passing ion density at transition minimum	1.7×10^{13} cm^{-3}
DT particle trapping current	800 A at each end
Hot ion density in anchor	7×10^{13} cm^{-3}
β_{anchor}	0.5
Plug	
Length	5.3 m
Passing ion density at barrier	4.7×10^{12} cm^{-3}
Trapped ion density at barrier	8.2×10^{12}
Sloshing ion density at barrier	9.4×10^{12}
Warm electron temperature at potential peak	124 keV
Hot electron energy at barrier	840
β_{plug}	0.5

REFERENCES

[1] B. Grant Logan, "Mirror Advanced Reactor Study (MARS)," Proc. of the ANS 5th Topical Meeting on Technology of Fusion Energy, Knoxville, TN, April, 1983.

[2] D. E. Baldwin, et al., "Studies in Tandem Mirror Theory," 8th Int. Conf. on Plasma Phys. and Cont. Nuclear Fusion Research, IAEA, Brussels, 1980, Vol. I, p. 133.

[3] L. D. Pearlstein, private communication (a users manual for TEBASCO will be published as a Lawrence Livermore National Laboratory UCRL report.

[4] D. E. Baldwin and B. G. Logan, editors, "Physics Basis for an Axicell Design for the End Plugs of MFTF-B," UCID-19359, Lawrence Livermore National Laboratory (Apr. 21, 1982), p. 10.

[5] D. E. Baldwin, Pumping of Thermal Barriers by Induced Radial Transport, Bull. Am. Phys. Soc. 26 (1981), 1021.

[6] D. E. Baldwin, "Pumping of Thermal Barriers by Inouced Radial Transport", Bull. Am. Phys. Soc. 26 (1981), 1021.

FIGURE CAPTIONS

Fig. 1. MARS tandem mirror reactor.

Fig. 2. MARS end-plug.

Fig. 3. Cross section of MARS central cell.

Fig. 4. MARS choke coils.

Fig. 5. (a) MARS end plug magnets. (b) corresponding axial profiles of filed $|B|(2)$ and potential $\phi(2)$ along the axis, and (c), corresponding $\phi(r,2)$ contours.

Fig. 6. MARS normal curvature.

Fig. 7. MARS geodesic curvature.

Fig. 8. Direct costs for MARS reactor plant equipment (1983 $).

Fig. 9. Minimum adiabatic length plugs allow smaller reactors (MINIMARS) compound to MARS.

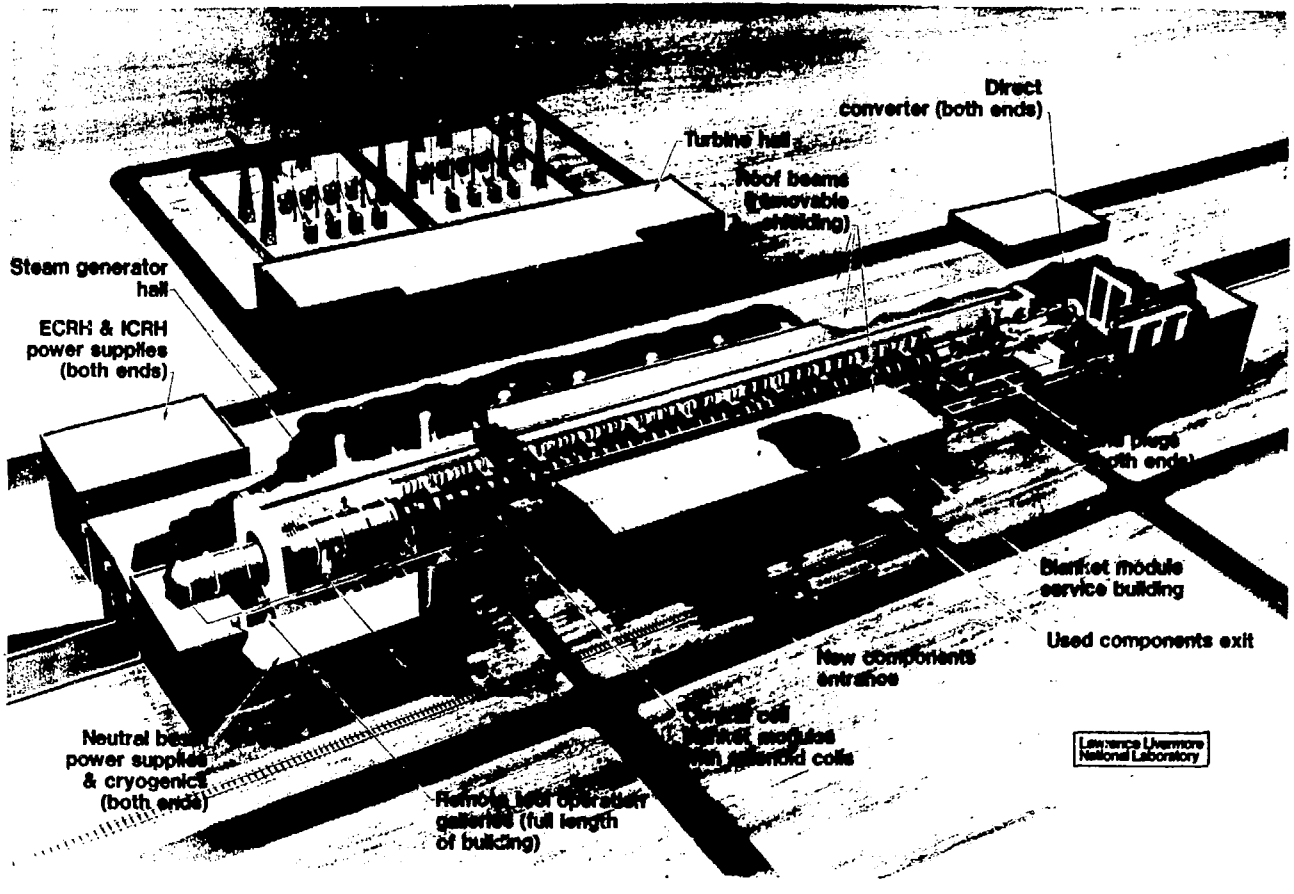

Fig. 1. MARS tandem mirror reactor.

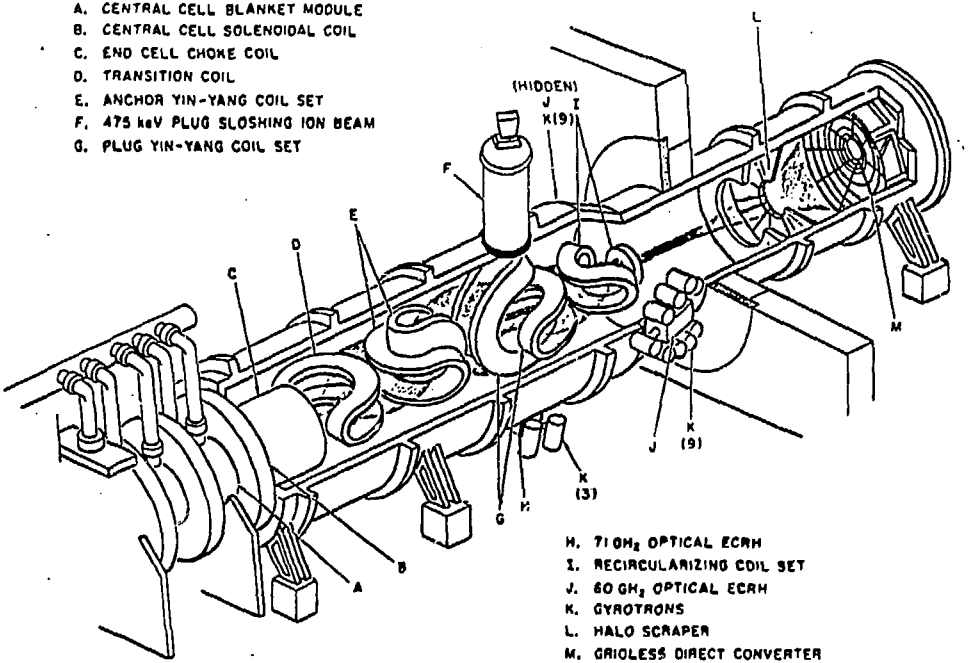

Fig. 2. MARS end-plug.

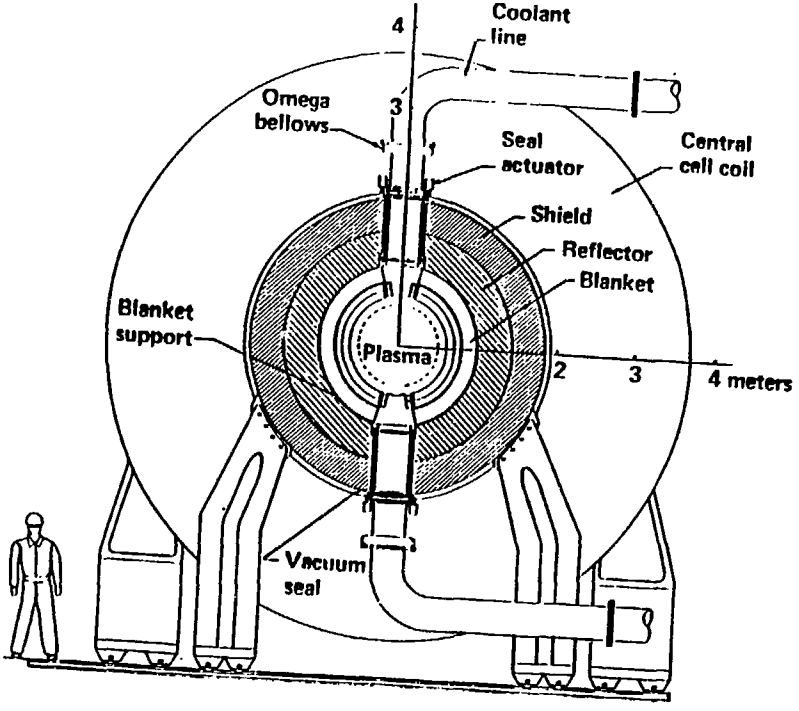

Fig. 3. Cross section of MARS central cell.

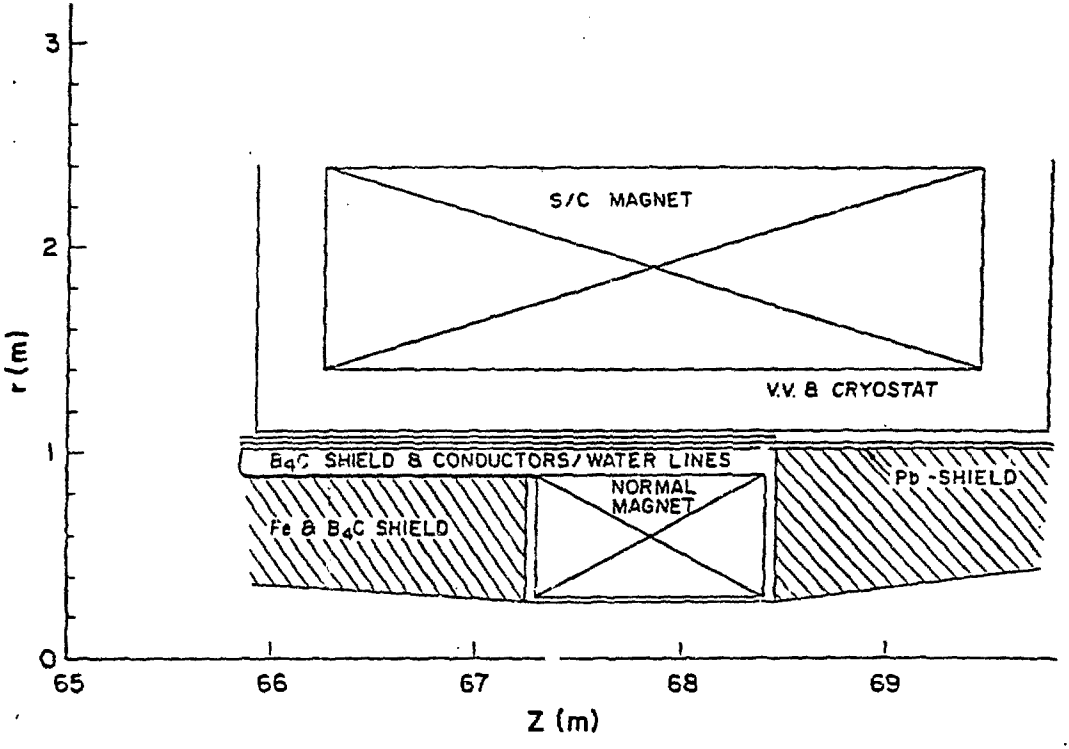

Fig. 4. MARS choke coils.

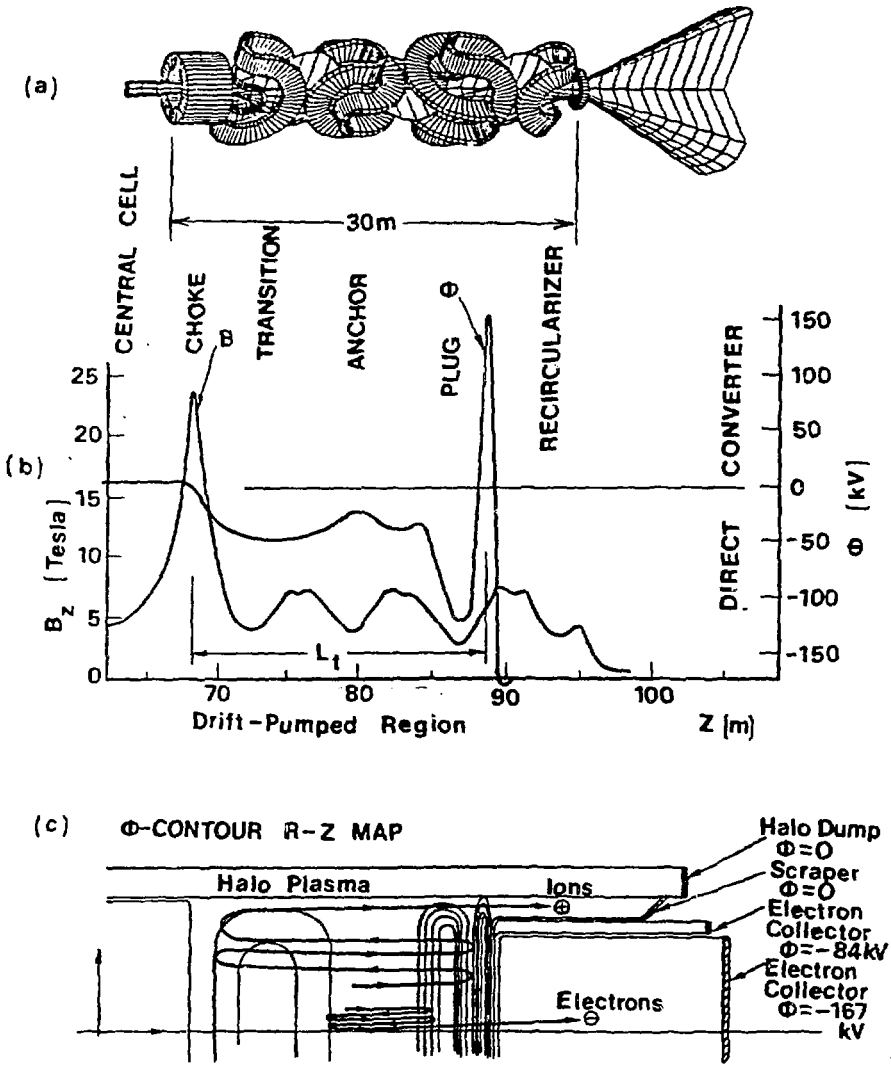

Fig. 5. (a) MARS end plug magnets. (b) corresponding axial profiles of filed $|B|(2)$ and potential $\phi(2)$ along the axis, and (c), corresponding $\phi(r,2)$ contours.

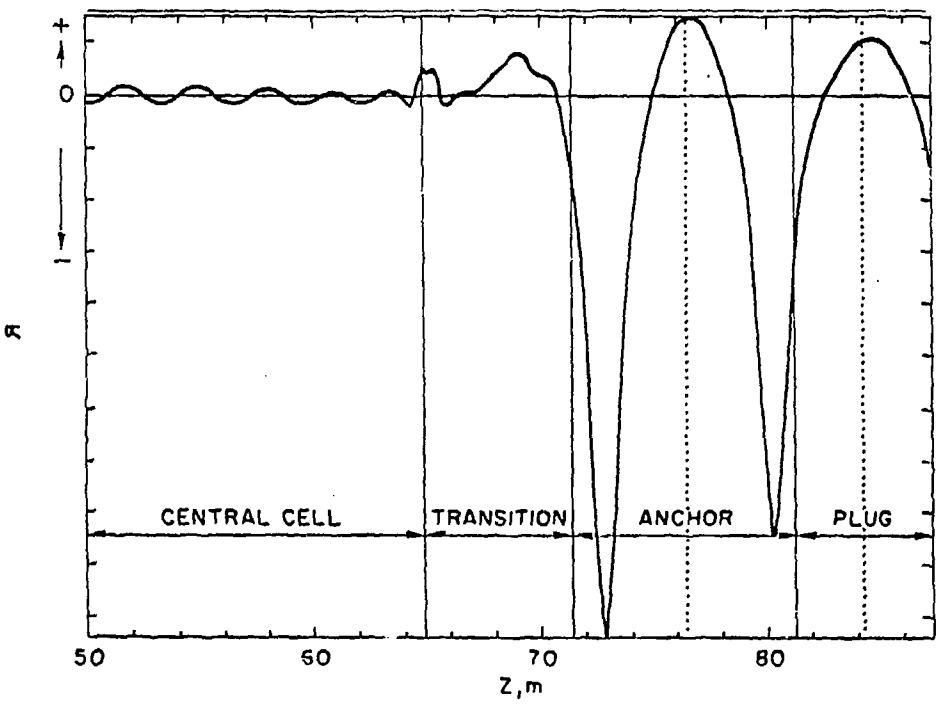

Fig. 6. MARS normal curvature.

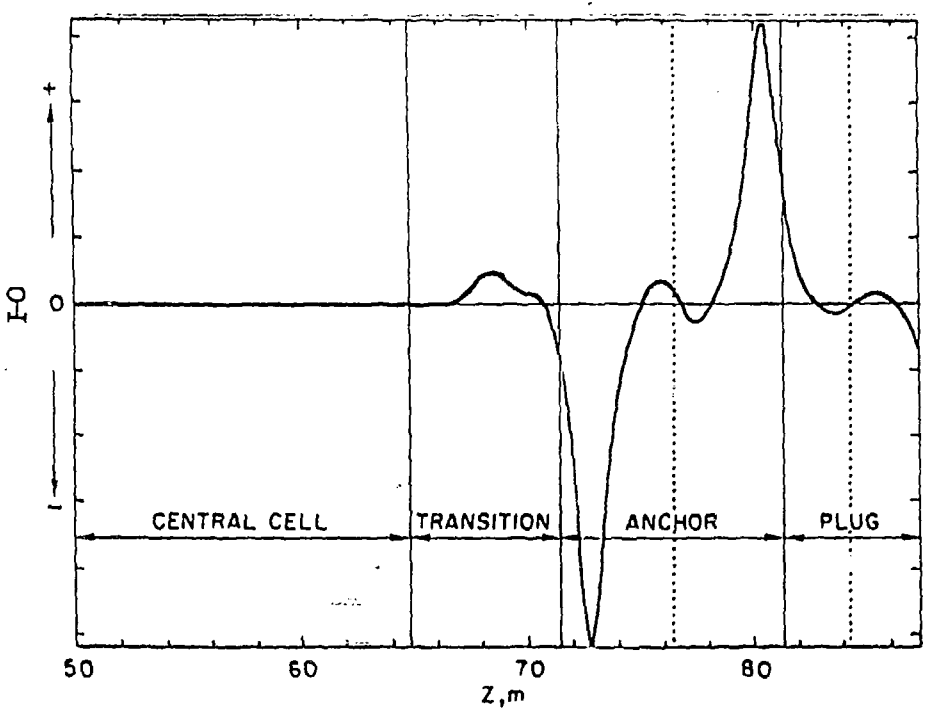

Fig. 7. MARS geodesic curvature.

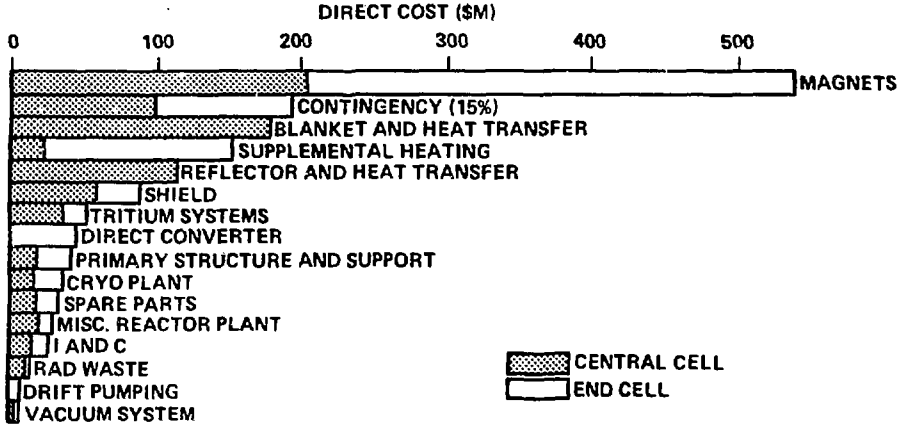

Fig. 8. Direct costs for MARS reactor plant equipment (1983 $). The total reactor plant direct cost is 1.52×10^9 $U.S.; the total power plant direct cost is 2.37×10^9 $U.S.

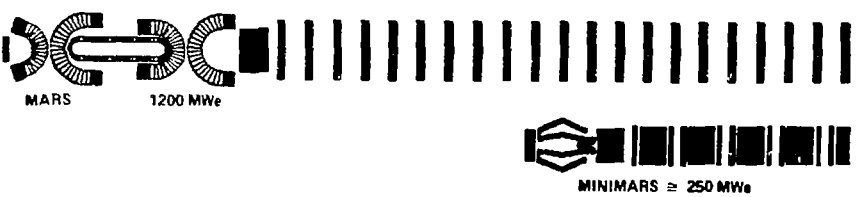

Fig. 9. Minimum adiabatic length plugs (≅ 8 m) allows smaller reactors (Minimars) compared to MARS.